PROCEEDINGS OF SCIENCE

# High-$p_{\rm T}$ dihadron and jet-hadron correlations in PbPb collisions measured by CMS

**Wei Li*** **on behalf of the CMS Collaboration**
*Massachusetts Institute of Technology*
*E-mail:* davidlw@mit.edu

We discuss recent results of the CMS experiment on high-$p_{\rm T}$ dihadron and jet-hadron correlations in PbPb collisions. The results were obtained for PbPb collisions at $\sqrt{s_{NN}} = 2.76\,TeV$ using tracks reconstructed in the CMS inner tracking system and fully reconstructed jets over a broad acceptance coverage. The results are presented as a function of collision centrality and compared to pp collisions at the same energy, allowing us to study the mechanism of parton energy loss in the QCD medium and to search for a possible medium response to the jet.

*The Seventh Workshop on Particle Correlations and Femtoscopy*
*September 20 - 24 2011*
*University of Tokyo, Japan*

*Speaker.



PoS(WPCF2011)028

# 1. Introduction

Measurements of dihadron azimuthal correlations have provided a powerful tool to study the properties of the strongly interacting medium created in ultrarelativistic nuclear collisions. An early indication of strong jet-medium interactions at RHIC was the absence of high-transverse-momentum (high-$p_{\mathrm{T}}$) back-to-back particle pairs in dihadron correlation measurements [1] and the corresponding enhancement of low-$p_{\mathrm{T}}$ hadrons recoiling from a high-$p_{\mathrm{T}}$ leading, or "trigger", particle [2]. The recent observations of asymmetric energies of reconstructed jets [3, 4] in PbPb collisions at the Large Hadron Collider (LHC) provide further evidence of jet quenching, suggesting a large energy loss for partons traversing the produced medium.

# 2. Results

## 2.1 Dihadron correlations

Dihadron correlations for charged particles have been measured extensively by the CMS experiment [5] in pp collisions at $\sqrt{s} = 7\,TeV$ [6] and PbPb collisions at a nucleon-nucleon center-of-mass energy ($\sqrt{s_{NN}}$) of $2.76\,TeV$ [7, 8] over a large phase space. The nearly $4\pi$ solid-angle acceptance of the CMS detector is ideally suited for studies of both short- and long-range particle correlations. The dihadron correlations analysis technique has been described in detail in Ref. [6, 7, 8].

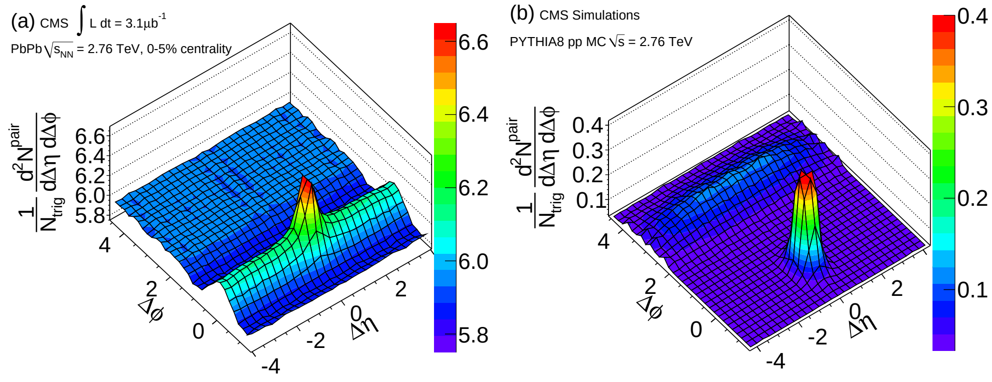


**Figure 1:** Two-dimensional (2-D) per-trigger-particle associated yield of charged hadrons as a function of $|\Delta\eta|$ and $|\Delta\phi|$ for $4 < p_{\mathrm{T}}^{\mathrm{trig}} < 6\,GeV/c$ and $2 < p_{\mathrm{T}}^{\mathrm{assoc}} < 4\,GeV/c$ from (a) 0–5% most central PbPb collisions at $\sqrt{s_{NN}} = 2.76\,TeV$, and (b) PYTHIA 8 pp MC simulation at $\sqrt{s} = 2.76\,TeV$.

The two-dimensional (2D) per-trigger-particle associated yield distribution of charged hadrons as a function of $|\Delta\eta|$ and $|\Delta\phi|$ is measured for each $p_{\mathrm{T}}^{\mathrm{trig}}$ and $p_{\mathrm{T}}^{\mathrm{assoc}}$ interval, and in different centrality classes of PbPb collisions. An example for trigger particles with $3 < p_{\mathrm{T}}^{\mathrm{trig}} < 3.5\,GeV/c$ and associated particles with $1 < p_{\mathrm{T}}^{\mathrm{assoc}} < 1.5\,GeV/c$ is shown in Fig. 2, for centralities ranging from the 0–5% most central collisions, to the most peripheral (70–80%) events. For the most central PbPb collisions, a clear and significant ridge-like structure mostly flat in $\Delta\eta$, and extending to the limit of $|\Delta\eta| = 4$, is observed at $\Delta\phi \approx 0$. At mid-peripheral events, a pronounced $\cos(2\Delta\phi)$ component emerges, originating predominantly from elliptic flow. In the most peripheral collisions, the ridge structure has largely diminished, while the away-side back-to-back jet correlations can be clearly seen at $\Delta\phi \approx \pi$, but spread out in $\Delta\eta$.

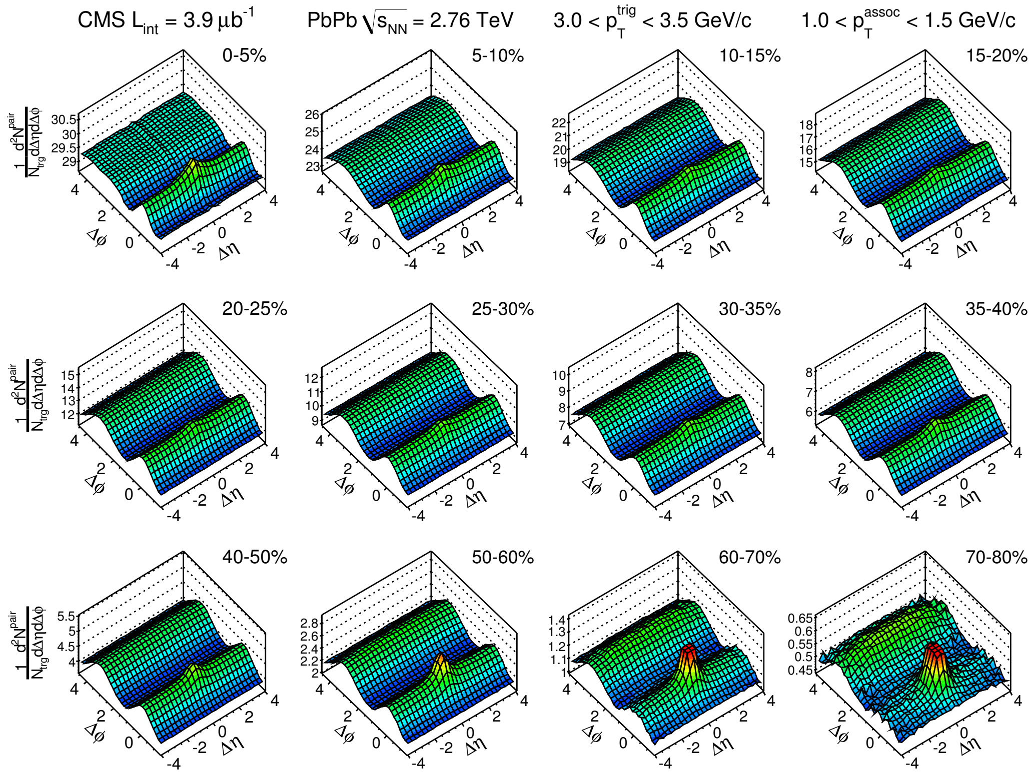


**Figure 2:** Two-dimensional (2D) per-trigger-particle associated yield of charged hadrons as a function of $|\Delta\eta|$ and $|\Delta\phi|$ for $3 < p_T^{trig} < 3.5\,GeV/c$ and $1 < p_T^{assoc} < 1.5\,GeV/c$, for twelve centrality ranges of PbPb collisions at $\sqrt{s_{NN}} = 2.76\,TeV$. The near-side peak is truncated in the two most peripheral distributions to better display the surrounding structure.

Figure 3 shows the integrated associated yields of the near-side peak and away-side regions as a function of $N_{part}$ in PbPb collisions at $\sqrt{s_{NN}} = 2.76\,TeV$, requiring $3 < p_T^{trig} < 3.5\,GeV/c$, for four different intervals of $p_T^{assoc}$. The pp results are represented using horizontal lines covering the full $N_{part}$ range. The yield of the near-side peak increases by a factor of 1.7 in going from the very peripheral 70–80% to the most central 0–5% PbPb events, for the lowest $p_T^{assoc}$ interval of 1–1.5 $GeV/c$. This is of particular interest because at RHIC energies for $p_T^{assoc}$ down to $2\,GeV/c$ and similar $p_T^{trig}$ ranges and methodology, although for a lower density system (AuAu at $\sqrt{s_{NN}} = 0.2\,TeV$), there is almost no centrality dependence observed. On both near and away sides, the yield in PbPb matches that in pp for the most peripheral events. On the away side, the yield in PbPb decreases with centrality, becoming negative for the most central events. The negative values of the yields in Fig. 3 are caused by a slightly concave structure on the away-side region ($1.18 < |\Delta\phi| < \pi$). The effect is more prominent for central PbPb events. Similar behavior was also observed at RHIC for AuAu collisions at $\sqrt{s_{NN}} = 200\,GeV$.

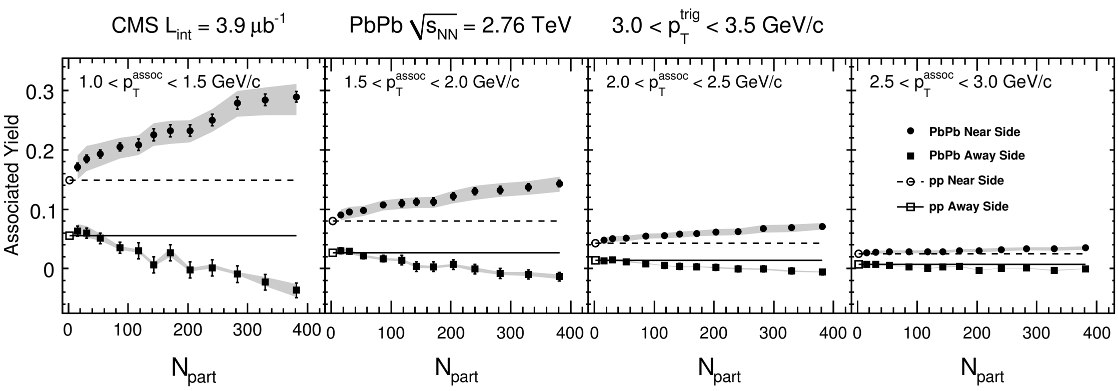


**Figure 3:** The integrated associated yields of the near-side peak ($|\Delta\phi| < 1.18$) and away-side region ($|\Delta\phi| > 1.18$), requiring $3 < p_T^{trig} < 3.5\,GeV/c$ for four different intervals of $p_T^{assoc}$, as a function of $N_{part}$ in PbPb collisions at $\sqrt{s_{NN}} = 2.76\,TeV$. The lines represent the pp results ($N_{part} = 2$) superimposed over the full range of $N_{part}$ values.

## 2.2 Jet-track correlations

The studies of calorimeter jets show a dramatic change of the jet momentum balance as a function of collision centrality. This implies a strong modification in the distribution of jet fragmentation products, with energy being either transported out of the cone area used to define the jets, or to low momentum particles to which the CMS calorimeter system is less sensitive [4].

To gain further insight on where the missing energy goes, the projection of missing $p_T$ onto the leading jet axis was determined for each event with a leading jet with $p_{T,1} > 120\ GeV/c$ and $|\eta_1| < 2$:

$$\not{p}_T^{\parallel} = \sum_{\text{Tracks}} -p_T^{\text{Track}} \cos\left(\phi_{\text{Track}} - \phi_{\text{Leading Jet}}\right).$$

The projected missing-$p_T$ parameter, $\not{p}_T^{\parallel}$, was calculated using all tracks with $p_T > 0.5\ GeV/c$ and $|\eta| < 2.4$, and then averaged over events to obtain $\langle \not{p}_T^{\parallel} \rangle$.

In the left panel of Fig. 4, $\langle \not{p}_T^{\parallel} \rangle$ is shown as a function of  for 0–30% PbPb collisions. Using tracks with $|\eta| < 2.4$ and $p_T > 0.5\ GeV/c$, one sees that indeed the momentum balance of the events, shown as solid circles, is recovered within uncertainties, for both centrality ranges and even for events with large observed dijet asymmetry, in data and simulation. The figure also shows the contributions to $\langle \not{p}_T^{\parallel} \rangle$ for different $p_T$ ranges from 0.5–1 $GeV/c$ to $p_T > 8\ GeV/c$. A large negative contribution to $\langle \not{p}_T^{\parallel} \rangle$ (i.e., in the direction of the leading jet) by the $p_T > 8\ GeV/c$ range is balanced by the combined contributions from the 0.5–8 $GeV/c$ regions.

Further insight into the radial dependence of the momentum balance can be gained by studying $\langle \not{p}_T^{\parallel} \rangle$ separately for tracks inside cones of size $\Delta R = 0.8$ around the leading and subleading jet axes, and for tracks outside of these cones. The results of this study for central events are shown in the middle and right panels of Fig. 4 for the in-cone balance and out-of-cone balance for MC and data.

One observes that for both data and MC an in-cone imbalance of $\langle \not{p}_{\rm T}^{\parallel} \rangle \approx -20$ $GeV/c$ is found for the $A_J > 0.33$ selection. In both cases this is balanced by a corresponding out-of-cone imbalance of $\langle \not{p}_{\rm T}^{\parallel} \rangle \approx 20$ $GeV/c$. However, in the data the out-of-cone contribution is carried almost entirely by tracks with $0.5 < p_{\rm T} < 4$ $GeV/c$ whereas in MC more than 50% of the balance is carried by tracks with $p_{\rm T} > 4$ $GeV/c$, with a negligible contribution from $p_{\rm T} < 1$ $GeV/c$.

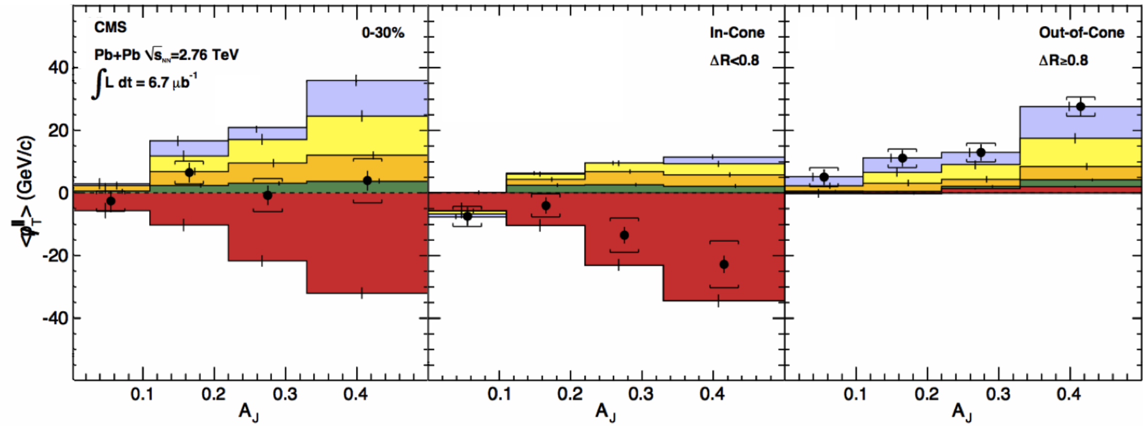


**Figure 4:** Left Panel: The $\langle \not{p}_{T}^{\parallel} \rangle$, for tracks with $p_{\rm T} > 0.5$ $GeV/c$, projected onto the leading jet axis (solid circles). The $\langle \not{p}_{T}^{\parallel} \rangle$ values are shown as a function of dijet asymmetry $A_J$ for $0-30\%$ central events. Middle Panel: The $\langle \not{p}_{T}^{\parallel} \rangle$ values as a function of $A_J$ inside $(R < 0.8)$ one of the leading or subleading jet cones. Right panel: $\langle \not{p}_{T}^{\parallel} \rangle$ outside $(R > 0.8)$ the leading and subleading jet cones.

To study a potential effect of parton energy loss on the fragmentation properties of partons in more detail, we divide the data sample into classes of dijet imbalance. Four $A_J$ bins are chosen that split the data sample into approximately equal parts: $0 < A_J < 0.13$, $0.13 < A_J < 0.24$, $0.24 < A_J < 0.35$, and $0.35 < A_J < 0.70$. The fragmentation functions are reconstructed separately for leading and subleading jets in pp and central PbPb events. Fig. 5 shows the fragmentation functions in bins of increasing dijet imbalance ($A_J$) from left to right (top row) and the corresponding ratio to the fluctuation convoluted pp reference (bottom row) [9]. For both leading and subleading jets, independent of the dijet imbalance bin, the PbPb fragmentation functions closely resemble those of the pp reference. This can be more directly seen from the bottom row of the figure, where the ratio of PbPb data to pp data is presented.

In summary, a comprehensive study of high-$p_{\rm T}$ dihadron and jet-hadron correlations in PbPb collisions at 2.76$TeV$ has been carried out by the CMS experiment at the LHC. From dihadron correlations, the near-side jet peak yield is enhanced from peripheral to the most central collisions. Jet-track correlation measurement is performed on PbPb events, where a large energy imbalance is observed for the QCD dijets. The data show that the calorimeter dijet imbalance is reflected in an imbalance in high $p_{\rm T}$ tracks above 8 $GeV/c$ in the direction of the leading jet. In central collisions, an increased balancing contribution of $p_{\rm T} < 1.5$ $GeV/c$ tracks is seen, which is not reproduced in the PYTHIA+HYDJET calculations. The fragmentation function of the reconstructed jets in PbPb collisions is found to resemble those of the pp collisions, independent of the dijet energy imbalance.

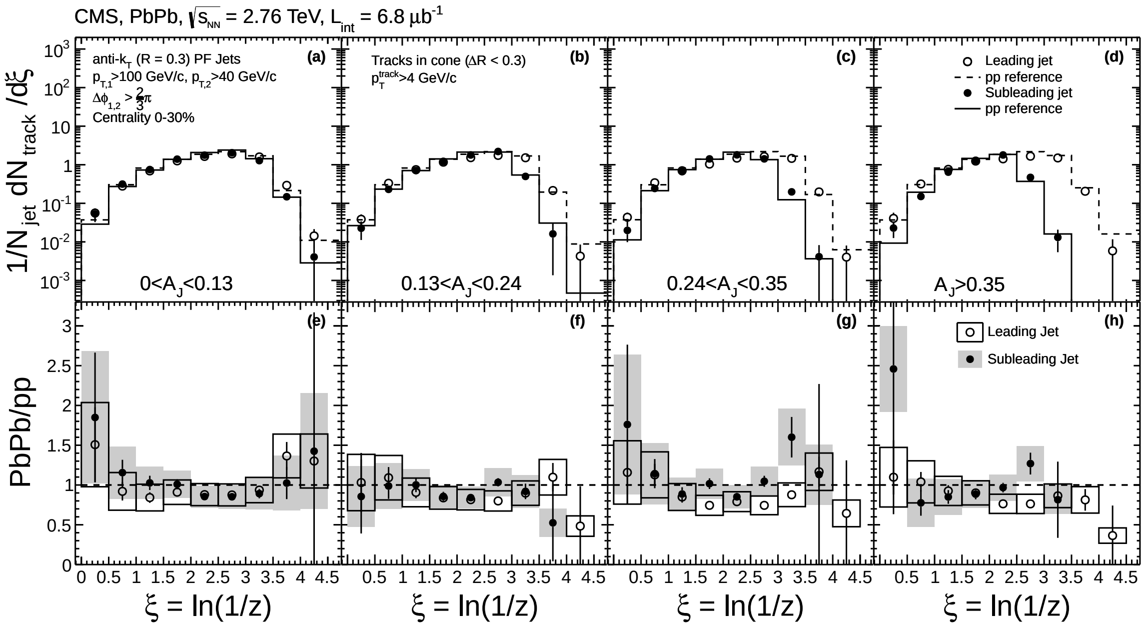


**Figure 5:** Fragmentation functions in $A_J$ bins, reconstructed in central PbPb and pp reference for the leading (open circles) and subleading (solid points) jets. The bottom row shows the ratio of each fragmentation function to its convoluted pp reference.

## References


[1] STAR Collaboration, *Phys. Rev. Lett.* **90**, 082302 (2003).

[2] STAR Collaboration, *Phys. Rev. Lett.* **95**, 152301 (2005).

[3] ATLAS Collaboration, *Phys. Rev. Lett.* **105**, 252303 (2010).

[4] CMS Collaboration, *Phys. Rev.* **C84**, 024906 (2011).

[5] CMS Collaboration, *JINST* **0803** S08004 (2008).

[6] CMS Collaboration, *JHEP* **09** 091 (2010),

[7] CMS Collaboration, *JHEP* **07**, 076 (2011).

[8] CMS Collaboration, *EPJC* **72**, 2012 (2012).

[9] CMS Collaboration, arXiv:1205.5872 [nucl-ex].